sustainability

*Supplementary material*

# Individual pattern response to $CO_2$-induced acidification stress in *Haliotis rufescens* suggests stage-specific acclimatization during its early life history

**Ricardo Gómez-Reyes [1], Clara E. Galindo-Sánchez [2], Fabiola Lafarga-De la Cruz [2], José M. Hernández-Ayón [2], Enrique Valenzuela-Wood [3] and Laura López-Galindo [3]***

To achieve the control of pH in seawater, a set of three water flow systems was assembled (Figure S1). Excluding the control bioassay (pH 8.0), independent pH controllers (AquaMedic, Germany) were calibrated using the National Bureau of Standards (NBS) and configured to maintain the water at the desired pH during the experiment to moderate (7.8) and low (7.6) pH levels, respectively. Pure $CO_2$ was injected using a ceramic $CO_2$ diffuser and mixed between the reservoirs (100 L) to drop and maintain the experimental water pH. The experimental seawater used during the bioassays was filtered (1 µm nominal-sized filter cartridges) and ultra-violet (UV) sterilized; the flux rate was maintained at 100 mL $min^{-1}$ in the experimental tanks. Additionally, a complete drain-off and refill with new experimental filtered seawater (FSW) were performed twice from the second reservoir during the bioassay. The FSW temperature was maintained (16 ± 0.6, mean ± S.E.) by setting the laboratory air conditioner to 16 °C.

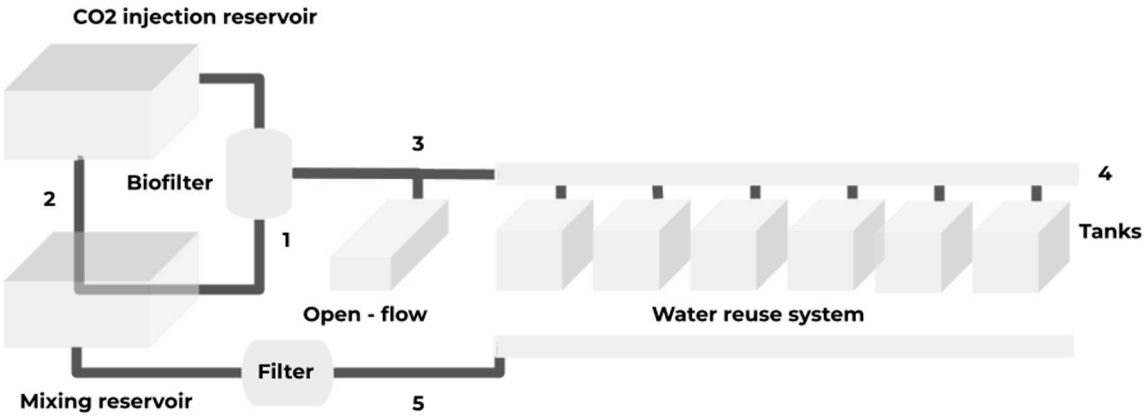


**Figure S1.** $CO_2$ injection system designed for the acidification with moderate (7.8) and low pH (7.6) challenges. These systems may contribute to water quality stabilization by managing the removal of solids and metabolism by-products (i.e., biofiltration) during larval development, including ammonia, and enabling control over gas transfer (i.e., $pCO_2$) and temperature. Numbers indicate water circulation. (1) Water is pumped from the mixing reservoir to the biofilter and $CO_2$ injection reservoir; then, (2) $CO_2$-mixed water goes back from the $CO_2$ injection reservoir to the mixing reservoir (20 L min -1). (3) Before hatching, the eggs are challenged to acidified water in a slow current open-flow system (5 mL min -1) maintained to the desired pH. (4) The $CO_2$-mixed water stream flows through six tanks (30 mL min -1, 28 x 11 x 10 cm), where

the hatched larvae are placed until the treatment ends. (5) Additional baffles and sieves with mesh sizes from 100 to 150 μm are included in the tanks to prevent the larvae from escaping when the reused water returns to the mixing reservoir system during the experiment.

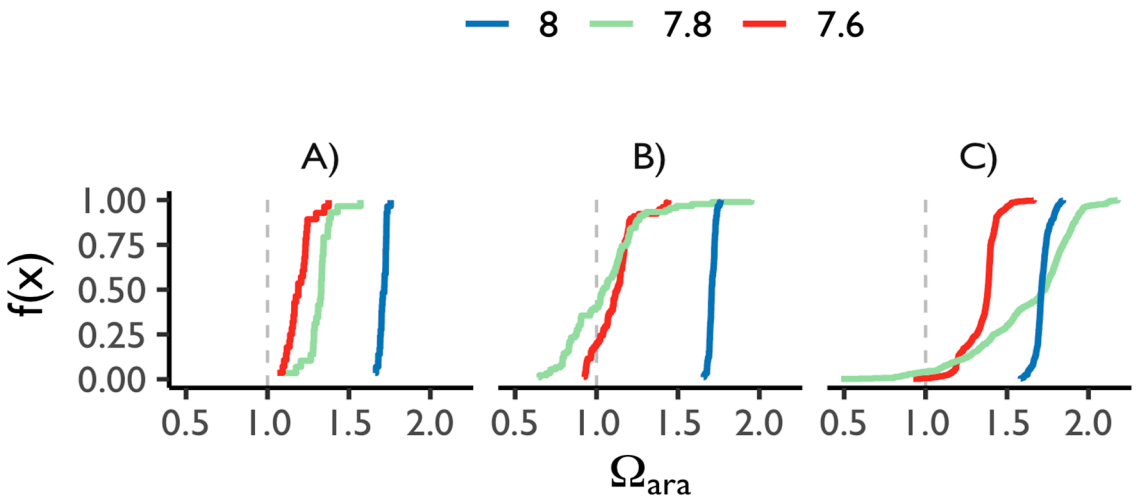


**Figure S2.** Empirical cumulative distribution (y axis) of predicted saturation levels of $CaCO_3$ with respect to aragonite (x axis) values obtained during the bioassay with the following pH conditions: control (pH 8.0, blue line), moderate (pH 7.8, green line) and low (pH 7.6, red line). **(A)** Before hatching, **(B)** during veliger maturation and **(C)** upon settlement (see top color legend for the acidification treatment). Values of $\Omega_{ara}$ below 1.0 (vertical dotted line in gray) represent an under-saturation level, meaning the water is corrosive. During veliger maturation and settlement, the haft and less than a quarter of the $\Omega_{ara}$ values were below this threshold for the pH challenges that mimic predicted near-future ocean acidification scenarios (green and red cumulative $\Omega_{ara}$ trends). The indices of the model performances were AIC: 26.073, BIC: 31.029, $R^2$ (adj.): 0.232, RMSE: 0.362 and Sigma: 0.467. The model was validated using the check_model function in the R package 'performance' version 0.7.2 (Lüdecke et al., 2021)[79].

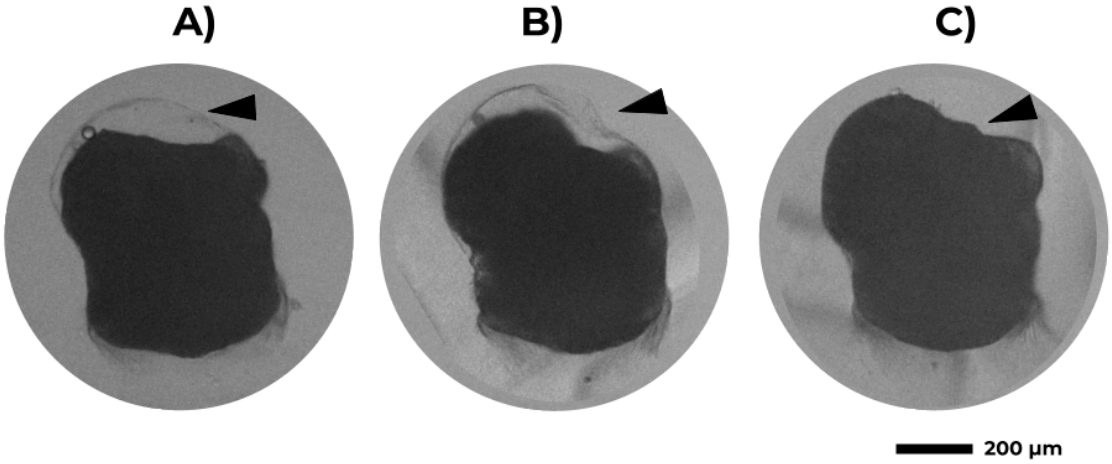


**Figure S3.** After 24 HPF, the shell first appears as a dome or cap on the posterior end of the larval body (black arrowhead). Individuals were scored as one of the possible morphological groups: **(A)** normal shelled, **(B)** abnormal shelled and **(C)** unshelled.

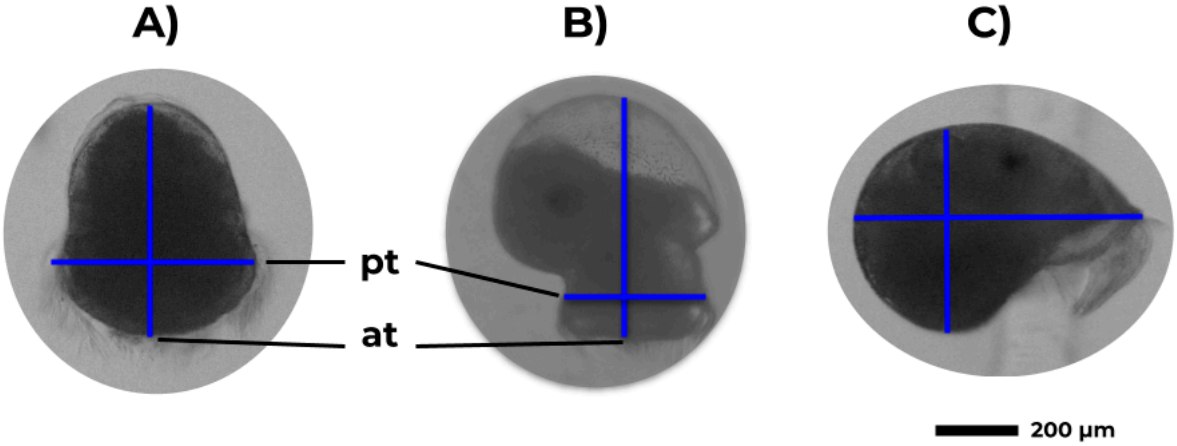


**Figure S4.** Morphological measurement of the width and length of larvae at 30, 48, 60 and 108 hours post fertilization (HPF). The presence of larvae observed at **30 HPF** include larvae with morphological features related to the trochophore stage **(A)** and early veliger stage **(B)**. Here, the measurement was made horizontally along the prototrochal ciliary band (pt) and vertically from the anterior apical tuft (at) towards the upper zone of the larvae. **(C)** Subsequent measurements at 48, 60 and **108 HPF** considered the maximum length and width of the shell. Images are not to scale.

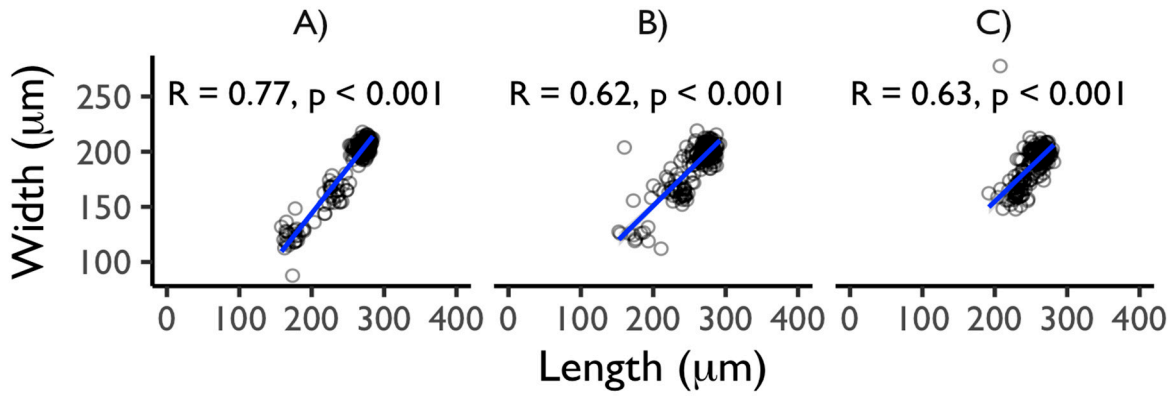


**Figure S5.** Morphometric assessment consisting of the width (x-axis) and the length (y-axis) during the abalone pelagic life history for **(A)** control (8.0), **(B)** moderate (7.8) and **(C)** low (7.6) pH. The larvae´s body widths and lengths are combined as a parameter to estimate growth using the square root product from the length x width. The Spearman correlation test was used for each treatment to calculate a monotonic relationship value (**R**).

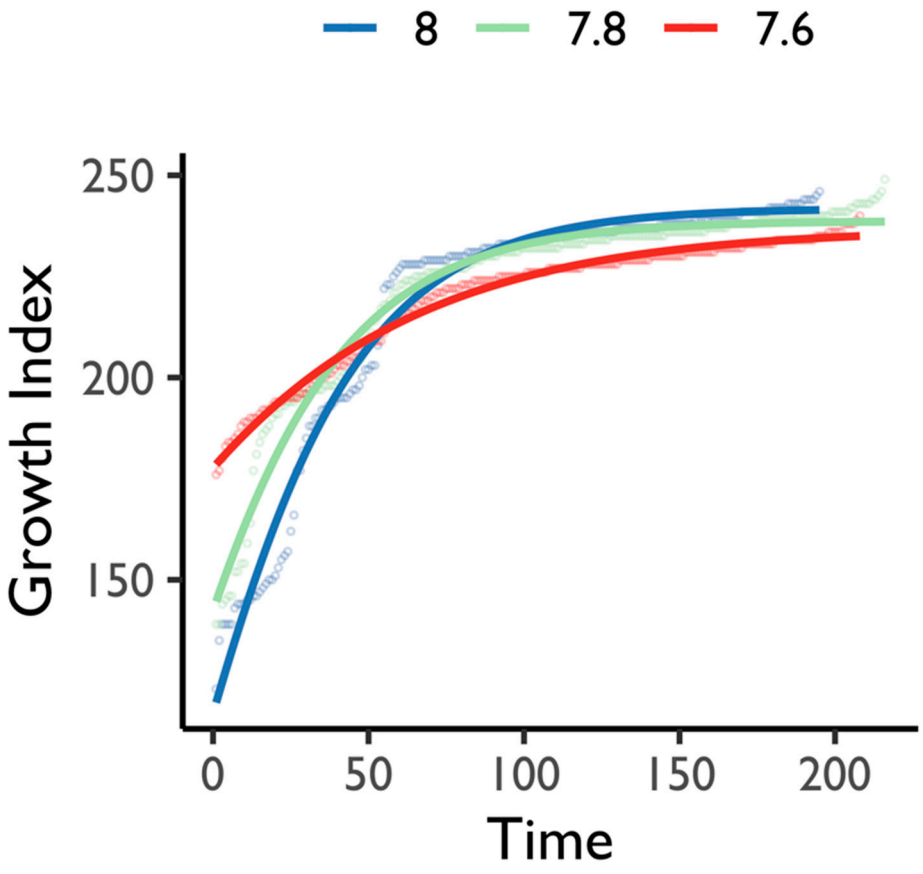


**Figure S6.** Length-at-stage analysis using Gompertz growth function: $ae^{-be^{-cx}}$.

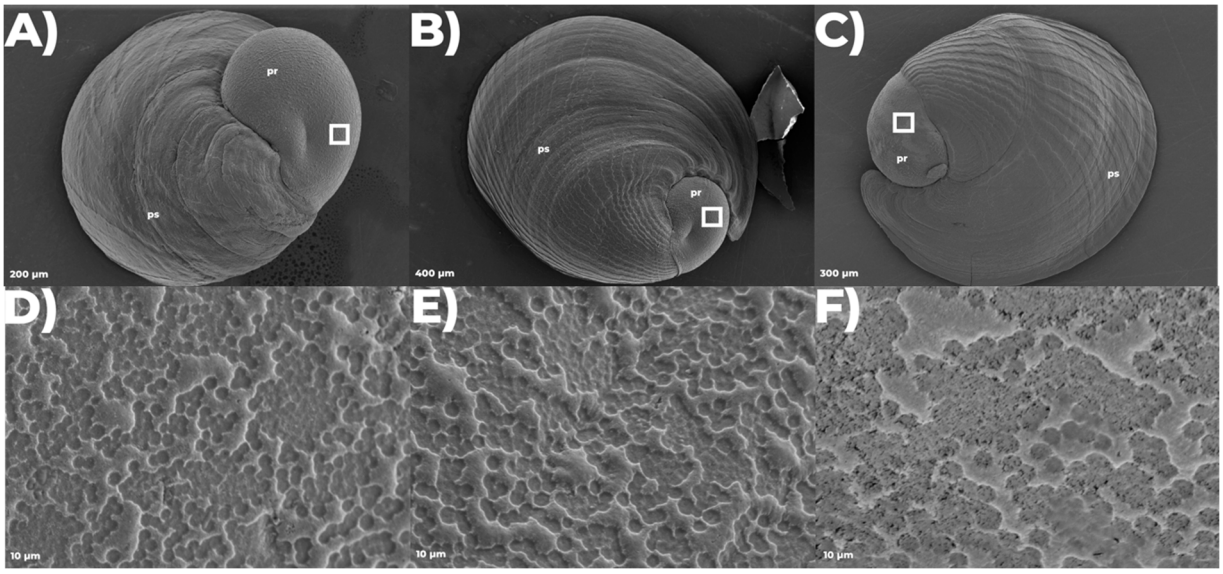


**Figure S7.** Scanning electron micrographs of *Haliotis rufescens* post-larvae reared under short-term acidification. Dorsal view (200 – 400 µm) of *Haliotis rufescens* 26-day-old post-fertilized larvae showing typical ear-shaped peristomal shell (**ps**) with growth rings and protoconch (**pr**). The control, moderate and low pH are shown, respectively (**A** – **C**). The laminar section (10 µm) from the protoconch (pr, white boxes, **A** - **C**) is observed in the bottom panel. No evidence of an abnormal granular texture along the protoconch nor microfractures was observed in all the experiments (**D** – **F**).

**Table S1.** Specific growth rate from Gompertz growth function: $ae^{-be^{-cx}}$.

| | **Control** | **Moderate** | **Low** |
|---|---|---|---|
| **Coefficient a** | 241.844 | 238.716 | 236.933 |
| **Coefficient b** | 0.726 | 0.516 | 0.288 |
| **Coefficient c** | 0.031 | 0.030 | 0.017 |
| **Specific growth rate (a*c)** | 7.532 | 7.258 | 4.040 |
| **Latency phase (b-1/c)** | -8.791 | -15.902 | -41.763 |
| **r-squared** | 0.977 | 0.974 | 0.988 |
| **Adjusted r-squared** | 0.977 | 0.973 | 0.988 |
| **AIC** | 1175.593 | 1205.052 | 818.517 |
| **BIC** | 1188.685 | 1218.553 | 831.867 |

**Table S2.** Predicted parameters derived from measured $pH_{NBS}$ records and in situ pH. The indices of model performances were AIC: 26.073, BIC: 31.029, $R^2$ (adj.): 0.232, RMSE: 0.362 and Sigma: 0.467. The model was validated using the check_model function in the R package 'performance' version 0.7.2 [79].

| Assay | Parameter | Stage | Mean ± SD | N records |
|---|---|---|---|---|
| **Low** | pH | Embryo | 7.5 ± 0.053 | 28 |
| **Moderate** | pH | Embryo | 7.7 ± 0.022 | 29 |
| | | | | |
| **Low** | pH | Veliger maturation | 7.4 ± 0.104 | 90 |
| **Moderate** | pH | Veliger maturation | 7.6 ± 0.066 | 90 |
| | | | | |
| **Low** | pH | Settlement | 7.7 ± 0.094 | 558 |
| **Moderate** | pH | Settlement | 7.8 ± 0.094 | 550 |
| **Control** | pH | Settlement | 8.1 ± 0.035 | 308 |
| | | | | |
| **Moderate** | Aragonite | Embryo | 1.32 ± 0.108 | 29 |
| **Control** | Aragonite | Embryo | 1.71 ± 0.022 | 29 |
| | | | | |
| **Low** | Aragonite | Veliger maturation | 1.12 ± 0.088 | 78 |
| **Moderate** | Aragonite | Veliger maturation | 1.05 ± 9.525 | 90 |
| **Control** | Aragonite | Veliger maturation | 1.71 ± 0.019 | 90 |
| | | | | |
| **Low** | Aragonite | Settlement | 1.35 ± 46.439 | 537 |
| **Moderate** | Aragonite | Settlement | 1.63 ± 0.233 | 543 |
| **Control** | Aragonite | Settlement | 1.72 ± 0.038 | 368 |
| | | | | |
| **Low** | pCO2_matm | Embryo | 930 ± 68.79 | 28 |
| **Moderate** | pCO2_matm | Embryo | 1020 ± 59.24 | 29 |
| **Control** | pCO2_matm | Embryo | 581 ± 5.38 | 29 |
| | | | | |
| **Low** | pCO2_matm | Veliger maturation | 1004 ± 115 | 78 |
| **Moderate** | pCO2_matm | Veliger maturation | 1229 ± 171 | 90 |
| **Control** | pCO2_matm | Veliger maturation | 582 ± 9 | 90 |
| | | | | |
| **Low** | pCO2_matm | Settlement | 778 ± 92.69 | 537 |
| **Moderate** | pCO2_matm | Settlement | 787 ± 233.02 | 543 |
| **Control** | pCO2_matm | Settlement | 580 ± 19.23 | 370 |